

# The Use Of A Multi-wavelength Lidar To Detect Aerosol Layers In The Atmosphere

Ferdinando De Tomasi <sup>1</sup> and Maria Rita Perrone <sup>1</sup>

<sup>1</sup>Dipartimento di Fisica, Università del Salento, Italy

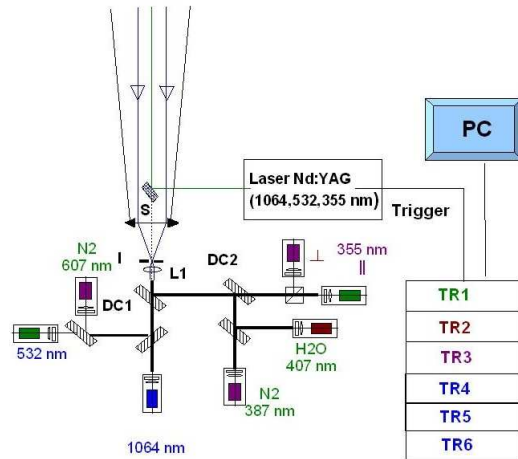


Figure 1. Sketch of the experimental apparatus. Legend: S: backscattered light from the atmosphere. I: Iris. L1: collimation lens. DCs: dichroic mirrors.

The lidar UniLe is operating at the Mathematics and Physics Department of Università del Salento since 1999 [1]. It is part of the European lidar network EARLINET since its foundation, in 2000, and it has been upgraded in 2010 to a multi-wavelength system. The experimental apparatus, shown in Fig. 1, is composed by a Nd:Yag laser operating at its fundamental wavelength, 1064 nm, and the second and third harmonic at 532 and 355 nm. The duration of the pulses are about 10 ns. The maximum energy per pulse is, when all harmonics are operative, respectively 1. J, 150 mJ and 300 mJ. The spatially separated laser beams are recomposed by a set of dichroic mirrors and sent vertically in the axis of a  $f/4$  Newton telescope. The backscattered radiation is collected by the primary mirror of the telescope and collimated by a plano-convex lens. The collimated beam is then sent into a polychromator where a selection of the wavelengths is operated by a set of dichroic mirrors and interference filters. Three different sections corresponding to the three laser wavelengths are identified. First, the UV section detects the elastic scattering from aerosol and atmospheric molecules and

the Raman scattering from N<sub>2</sub> and H<sub>2</sub>O. Furthermore, the elastic scattering is splitted by a non polarising cube: the transmitted beam is detected, and the reflected beam is filtered by a plate polarizer to detect only the cross-polarized component. Thus, in the UV section, the system can measure the volume depolarization of the atmosphere at 355 nm, the backscattering coefficient, the extinction coefficient at 355 nm exploiting the Raman scattering from N<sub>2</sub>, and the mixing ratio of water vapour. The green section

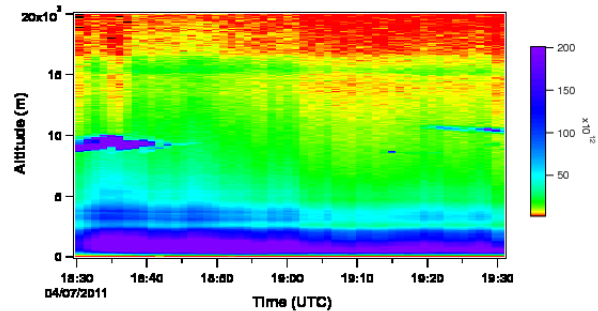


Figure 2. Logarithmic color map (arbitrary units) of the range-corrected signal at the 532 nm laser wavelength. Different features can be observed: two separate layers at altitude lower than 5000 m, cirrus clouds at about 10000 m and a stratospheric aerosol layer above 15000 m.

detects the elastic scattering from the laser radiation at 532 nm and its inelastic component at 607 nm, so that backscattering and extinction at these wavelengths can be retrieved. The infrared part detect simply the elastic backscattering at 1064 nm, being the Raman scattering at 1064 nm too small to be detected in normal conditions. The 1064 signal is detected by an avalanche photodiode; all the other signals are detected by photomultipliers. Finally, the signals are sent to transient recorders that have both a 12 bit A/D conversion and a photon counting capability. In this way the full dynamic range of the signals can be covered gluing the A/D signal from low altitudes to the PC signals from higher

altitudes in a range in which the signals are respectively above the noise threshold and below the saturation level. The H<sub>2</sub>O and the 1064 signals are respectively detected by single PC and A/D transient recorder ( the H<sub>2</sub>O Raman signal is usually low enough to avoid saturation and the photodiode used to detect 1064 does not detect single photons ). Usually the transient recorders integrate over 2000 laser shots that correspond to about 60 s. The lidar is located in the Depart-

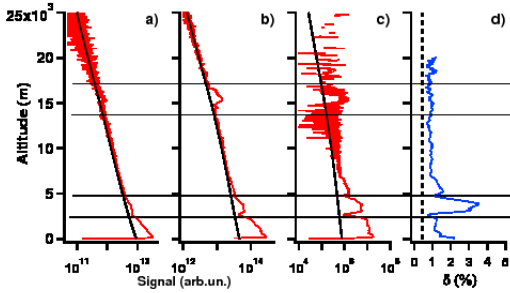


Figure 3. a-c) Averaged range-corrected lidar signals (logarithmic scale) at the three laser wavelengths, corresponding to cloud-free time intervals of Fig. 2. In black, the signal from a pure molecular atmosphere calculated by radiosoundings and a model ( MSIS of NASA). d) Volume depolarization at 355 nm. The dashed line is the value of the depolarization from the aerosol free atmosphere. The black horizontal lines are a guide for the eye evidencing the layers in the atmosphere.

ment, in a rural environment ( 40.33 N, 18.11 E ). We present here a case study in which different atmospheric layers are detected and can be discriminated by the multi-wavelength LIDAR. Figure 2 shows a color map (logarithmic) of the range corrected elastic signal at 532 nm acquired on July 4, 2011, between 18:30 and 19:30 UTC. Such images are useful for a quick-look of the signals and evidenciate the main features of the atmospheric scattering. Also, such images are useful to identify temporal intervals in which the signals look homogeneous, so that they can be temporally averaged to improve the S/N ratio. It is possible to deduce from this quicklook image: 1) a low altitude layer, possibly corresponding to a local Planetary Boundary Layer (PBL) and a residual layer up to 2500 m. 2) a medium altitude layer from 2500 to 5000 m 3) an high altitude layer at stratospheric altitude (larger than 15000 m). At the beginning and at the end of the acquisition a strong backscattering can be observed at altitudes about 10000 m. This is typically a sig-

nature of cirrus clouds, as confirmed by the high depolarization (not shown here).

If we average the signals in the intervals corresponding to the absence of clouds, we obtain the elastic signals shown in Fig.3, where the aerosol layers are evidenced. The depolarization measurements are also shown in the figure. On the basis of the signals and the depolarization measurements, we can identify three main layers: a low-depolarizing layer at low altitudes, an high-depolarizing layer in the middle troposphere, and another low-depolarizing layer in the high troposphere. Furthermore, a peak in the signals around 17000 m is displayed in each of the elastic signals, indicating the presence of stratospheric aerosol. In the figure, simulated signals corresponding to an aerosol free atmosphere are also shown. These simulated signals are necessary to identify ranges of altitudes that can be considered aerosol-free for calibration purposes. Also, a lidar signal that reduces to a pure molecular signal at high altitude is a proof that the system is working properly.

A first quantitative analysis of the signals is the calculation of backscattering coefficient. This is done by standard methods[2], using a constant lidar ratio  $S = 50$ . At 355 and 532 nm the calibration is made by a fit of the lidar signal at the molecular signal in the interval 25000-30000 m. At 1064 nm, it is not possible to apply this technique because of the high altitude of the aerosol free region and not enough S/N ratio at this altitude, thus a method relying on the cirrus backscattering has been used [3].

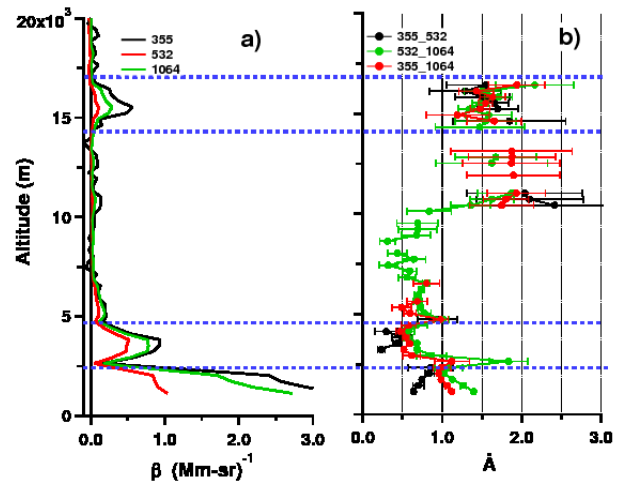


Figure 4. a) Aerosol backscattering coefficient for the three wavelengths. b) Angstrom coefficient for the different wavelengths pair. Error bars represent the statistical error. Blue horizontal lines are a guide for the eye evidencing the layer of the atmosphere.

From the backscattering it is possible to estimate the extinction and then calculate the Angstrom coefficient, which is defined by the relationship:

$$\mathring{A}_{\lambda_1-\lambda_2} = -\frac{1}{\ln\left(\frac{\lambda_1}{\lambda_2}\right)} \ln\left(\frac{\alpha_{\lambda_1}}{\alpha_{\lambda_2}}\right) \quad (1)$$

where  $\alpha$  is the extinction,  $\alpha = S\beta$ .

Figure 4 shows the backscattering coefficient at the three laser wavelengths and the angstrom coefficient for the wavelengths pairs. Only points that satisfy the following conditions are reported: if the value is larger than 0.1, the relative error must be minor than 0.5; if the value is less than 0.1, the absolute error must be lower than 0.3. Larger errors correspond obviously to region in which the backscattering coefficient is low. We can see that Angstrom coefficient is different for the different layers: the lower layer has an average  $\mathring{A} = 1$ , the second is instead significantly much lower (0.5). In the stratosphere, above 10000 m the Angstrom coefficient become higher, around 1.5-2. In the layer corresponding to the aerosol stratospheric peak, it is possible to see that the statistical error reduces (because of the increased backscattering) and sets to a value of 1.5.

From the discussion above, it is possible to conclude that two main tropospheric layers and one stratospheric layer are present. To assess the origin of these air masses, all available information should be used. Usually, dust particles have high depolarization and a low Angstrom coefficient, so that it is highly probable that the second layer is composed by dust. The lowermost layer has a lower depolarization and an higher angstrom coefficient so that it seems decoupled from the higher one. A comparison with analytical backtrajectories, not shown here, show that the higher layer actually originates from Sahara region and the lower altitude particles are down-lofted from higher altitudes. These air masses could be loaded with aerosol produced in forest fires in North-America. Finally, the stratospheric layer must be discussed. This layer is characterized by a very low volume depolarization and an higher Angstrom coefficient, which indicates small, nearly spherical particles. Actually, stratospheric aerosol are usually produced by volcanic eruptions, that emits SO<sub>2</sub> that is converted to H<sub>2</sub>SO<sub>4</sub> that can origin sulphates particles. In this period, actually, an eruption has been reported for the Nabro volcano in Eritrea. The eruption has been active between June and July 2011. Stratospheric aerosol have been observed in many stations in the world during this period, and also from the satellite lidar CALIPSO, so that it is very like that the observed peak is due to a volcanic plume [4].

## REFERENCES

1. F. De Tomasi and M.R. Perrone, Journal of Geophysical Research-Atmospheres 108,(2003) 10.1029/2002jd002781.
2. C. Weitkamp (ed.), Lidar. Range resolved remote sensing of the atmosphere", Springer Series in Optical Sciences, vol 102, (2005).
3. F. Navas-Guzman *et al.*, Opt. Pura Apl., 44,(2011) pp 49-53.
4. P. Sawamura *et al.*, Environmental Research Letters 7 (2012),034013 (9 pp).